DOI: 10.1002/adma.201706785

Article type: Communication

Oriented Nanofibrous Polymer Scaffolds Containing Protein-loaded Porous Silicon Generated by Spray Nebulization

By Jonathan M. Zuidema[||], Tushar Kumeria[||], Dokyoung Kim, Jinyoung Kang, Joanna Wang, Geoffrey Hollett, Xuan Zhang, David S. Roberts, Nicole Chan, Cari Dowling, Elena Blanco-Suarez, Nicola J. Allen, Mark H. Tuszynski, and Michael J. Sailor*

[*] Prof. M. J. Sailor, Dr. J.M. Zuidema, Dr. T. Kumeria, D. S. Roberts, X. Zhang, N. Chan

Department of Chemistry and Biochemistry
University of California, San Diego

9500 Gilman Drive, La Jolla, CA, 92093 (USA)
E-mail: msailor@ucsd.edu

Dr. T. Kumeria

School of Pharmacy

University of Queensland

20 Cornwall Street, Woolloongabba, Brisbane, Queensland 4102, Australia

Prof. D. Kim

Department of Anatomy and Neurobiology

College of Medicine

This is the author manuscript accepted for publication and has undergone full peer review but has not been through the copyediting, typesetting, pagination and proofreading process, which may lead to differences between this version and the Version of Record. Please cite this article as doi: 10.1002/adma.201706785.

This article is protected by copyright. All rights reserved.

Author Manuscript

Submitted to ADVANCED MATERIALS

Kyung Hee University

26 Kyungheedae-Ro, Dongdaemun-Gu, Seoul 02447, Republic of Korea

J. Kang

Department of Nanoengineering

University of California, San Diego

9500 Gilman Drive, La Jolla, CA 92093 (USA)

J. Wang, G. Hollett

Materials Science and Engineering

University of California, San Diego

9500 Gilman Drive, La Jolla, CA, 92093 (USA)

Prof. N.J. Allen, C. Dowling, Dr. E. Blanco-Suarez

Molecular Neurobiology Laboratory

Salk Institute for Biological Studies

10010 N Torrey Pines, La Jolla, CA, 92037 (USA)

Prof. M.H. Tuszynski

Veterans Administration Medical Center

3350 La Jolla Village Drive, San Diego, CA, 92161 (USA)

Prof. M.H. Tuszynski

Department of Neurosciences

University of California, San Diego

Author Manuscript

This article is protected by copyright. All rights reserved.

222222242

9500 Gilman, La Jolla, CA 92093 (USA)

Author Manuscript

Keywords: rat ganglion cells, photoluminescence, controlled release drug delivery, protein therapeutics, cell guidance, airbrush, lysozyme, biologics, polycaprolactone, PLA, poly(lactide-*co*-glycolide), PLGA, time-gated photoluminescence imaging, tissue engineering.

ABSTRACT

Oriented composite nanofibers consisting of porous silicon nanoparticles (pSiNPs) embedded in a polycaprolactone (PCL) or poly(lactide-*co*-glycolide) (PLGA) matrix are prepared by spray nebulization from chloroform solutions using an airbrush. The nanofibers can be oriented by appropriate positioning of the airbrush nozzle, and they can direct growth of neurites from rat dorsal root ganglion neurons. When loaded with the model protein lysozyme, the pSiNPs allow the generation of nanofiber scaffolds that carry and deliver the protein under physiologic conditions (PBS, 37°C) for up to 60 days, retaining 75% of the enzymatic activity over this time period. The mass loading of protein in the pSiNPs is 36%, and in the resulting polymer/pSiNP scaffolds it is 2.5%. The use of pSiNPs that display intrinsic photoluminescence (from the quantum-confined Si nanostructure) allows the polymer/pSiNP composites to be definitively identified and tracked by time-gated photoluminescence imaging. The remarkable ability of the pSiNPs to protect the protein payload from denaturation, both during processing and for the duration of the long-term aqueous release study, establishes a model for the generation of biodegradable nanofiber scaffolds that can load and deliver sensitive biologics.

Polymer nanofibers have been developed as scaffolds for numerous tissue engineering and nervous system repair applications due to their ability to mimic the topographical features of the extracellular environment and release a therapeutic payload at the target site.[1-8] However, they still remain largely irrelevant in the clinic.[9-10] This is in part due to the difficulty of readily fabricating nanofiber scaffolds that can deliver proteins or other biologics capable of stimulating tissue repair and regeneration. The vast majority of nanofibers are created using an electrospinning method, where an electric force is used to draw a polymer solution to a charged collector.[11] While this technique has shown utility in fabricating both randomly oriented and aligned nanofibers, there are

This article is protected by copyright. All rights reserved.

two key drawbacks with this approach: (1) the fibers can only be fabricated on a surface in contact with the charged collector; and (2) polymer nanofibers are generally fabricated by dissolving the polymer in an organic solvent, making it difficult to load and retain the activity of biologics for extended release drug delivery applications.[12]

The most common method used to include sensitive biologics in polymer nanofibers is coaxial electrospinning, where a spinneret composed of two coaxial capillaries is used instead of a single nozzle.[13] Two solutions are fed through the inner/outer capillaries forming a compound droplet at the exit of the spinneret. When loading sensitive biologics, the inner core is commonly an aqueous solution containing proteins, DNA or oligonucleotides of interest. The outer shell is then formed from a hydrophobic polymer solution.[14] While coaxial electrospinning has substantial advantages, the process still has several drawbacks. These include: (i) instability of sensitive biological agents due to the high voltage, shearing forces at the core/shell interface, and rapid protein dehydration, (ii) increased difficulty in obtaining consistent nanofibers due to multiple phases, and (iii) inability to deposit nanofibers directly onto a surface of interest. However, nanoscale polymer fibers have led to improved outcomes in the development of tissue engineering scaffolds, stem cell differentiation, and *in vitro* cell culture environments that more closely resemble the *in vivo* milieus they are modeling. [15-22] Therefore, creating more versatile and readily fabricated polymer nanofibers that can elute biologic therapeutics and stimulate cellular growth is a key need for the successful translation of nanofiber tissue scaffolds to the clinic.

Mesoporous silicon is a biodegradable inorganic material that has been extensively investigated for photoluminescence-based imaging and drug delivery applications.[23-25] The biocompatibility and degradability of mesoporous silicon nanoparticles (pSiNPs) has been demonstrated *in vivo*.[26-27] The mechanism of dissolution of porous silicon (pSi) under *in vivo*

Author Manuscript

This article is protected by copyright. All rights reserved.

conditions involves oxidation of silicon to form silicon oxide, followed by hydrolysis of the resulting oxide phase into water-soluble orthosilicic acid ($Si(OH)_4$).[28] The high porosity of pSiNPs inherently provides a large pore volume to load therapeutics, which are delivered as the pSi skeleton degrades.[29-32] This degradation leads to changes in the intrinsic photoluminescent properties of pSi, which have been harnessed to provide a self-reporting drug delivery feature.[33] Of particular relevance to the present work, pSi has been shown to be capable of loading and protecting various sensitive biologics from proteolytic or nucleolytic degradation,[34-36] and it has been incorporated into a wide range of biomedically relevant polymer systems,[37-42] and larger, micron-scale particles of pSi have previously been incorporated into PCL-based scaffolds.[43-48] Most recently, a pSi host has been shown to afford protection to the protein lysozyme against degradation by non-aqueous solvents, providing a means to protect proteins from non-aqueous media.[36] Here we report a facile nebulization process that combines protein-loaded pSiNPs into polymer nanofibers and coats them onto uncharged surfaces. We find these hybrid nanofibers can guide cellular growth, exhibit photoluminescence, and release bioactive proteins (Scheme 1).

Author Manuscript

This article is protected by copyright. All rights reserved.

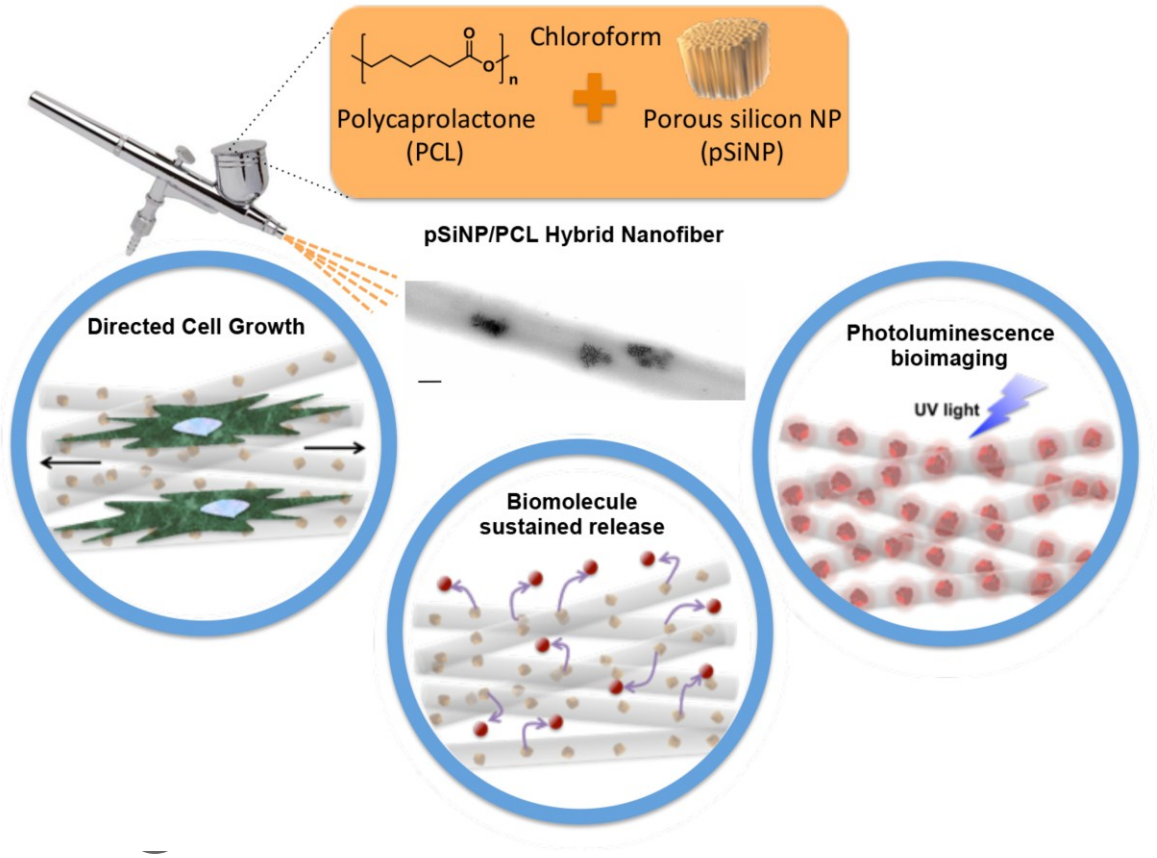

Scheme 1. Spray nebulization is used to produce nanofibers of polycaprolactone embedded with porous silicon nanoparticles (pSiNPs). The polymer fibers can direct cell growth, and the entrapped pSiNPs display an intrinsic photoluminescence that can be used to track degradation of the composite polymer/pSiNP scaffold. Although proteins are generally not soluble in or compatible with chloroform, the pSiNPs can sequester and protect a protein payload, allowing active protein to be co-formulated with the biodegradable polymer.

Spray nebulization of chloroform solutions 4% (*w*/*w*) of polycaprolactone (PCL) or 10 % (*w/w)* poly(lactide-*co*-glycolide) (PLGA) by means of an airbrush[49] generated polymer nanofibers [Figure S1, Supporting Information]. The deposition distance and spraying angle were optimized to control fiber morphology, diameter, and alignment. We found that a distance of 20 cm from the airbrush nozzle to the collector reproducibly produced well-defined PCL nanofibers [Figure S2, Movie S1, Supporting Information]. Similar nanofibers (average diameter: 580–590 nm) could be

Author M

This article is protected by copyright. All rights reserved.

generated using PLGA as the polymer source [Table S1, Supporting Information]. In order to prepare aligned fibers, the stream of material ejected from the airbrush nozzle was adjusted to strike the plane of the collector (typically, a glass microscope slide) at a 20° angle. Adjustment of this angle and the distance between the nozzle and the collector allowed optimization of the nanofiber morphology and degree of alignment [Figure S2, S3, Movie S2, Supporting Information].

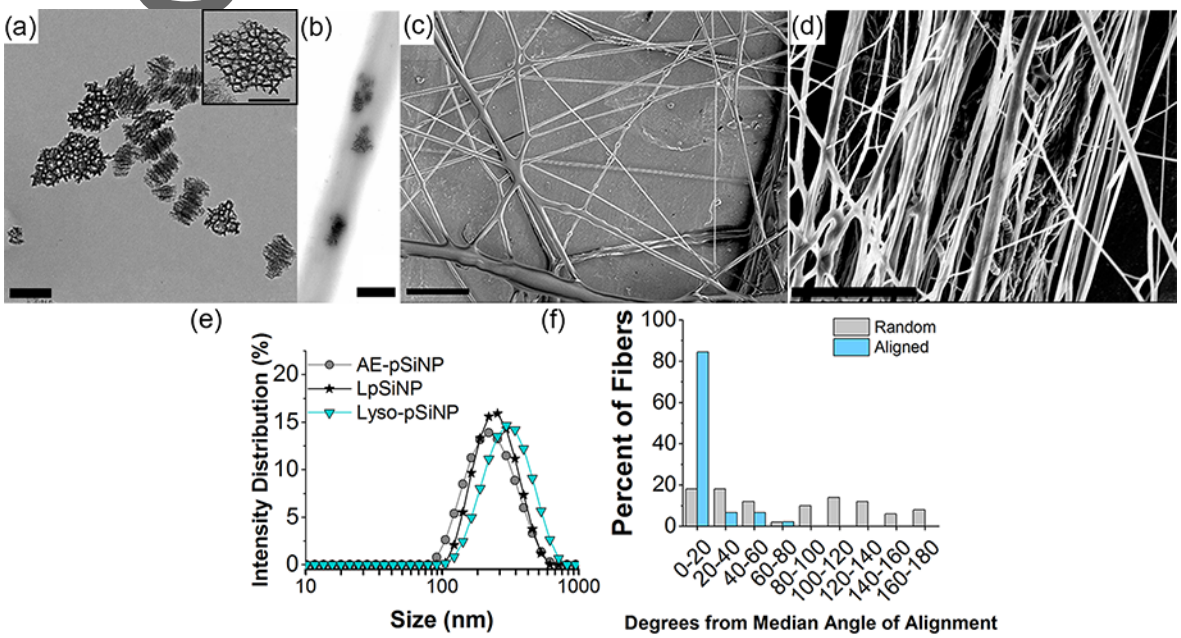

Figure 1. Transmission electron microscope (TEM) image of (a) as-etched pSiNP (Scale = 200 nm, inset scale = 100 nm) and (b) hybrid nanofiber showing embedded as-etched-pSiNPs (scale = 400 nm). Scanning electron microscope images of (c) non-aligned (scale = 10 μm), and (d) aligned hybrid nanofibers (scale = 5 μm). (e) Size distribution of different pSiNP formulations measured by DLS. AE-pSiNP is as-etched porous silicon nanoparticles; LpSiNP is photoluminescent porous silicon nanoparticles (prepared by borate oxidation); Lyso-pSiNP is porous silicon nanoparticles loaded with lysozyme. (f) Quantification of angular orientation of fibers comparing non-aligned (Random) with uniaxially aligned (Aligned) hybrid nanofibers, created by spray nebulization. These PCL fibers contained as-etched pSiNPs as described in the text.

Author Manuscript

This article is protected by copyright. All rights reserved.

We next tested the spray nebulization method to assess if it would allow the incorporation of pSiNPs into the fibers. To prepare composites of the nanofibers with pSiNPs, as-etched nanoparticles prepared with a mean diameter of 210 nm [Table S2, Supporting Information] and nominal porosity of 46 ±2% were suspended in a chloroform solution containing 4% PCL and 0.2% pSiNPs by mass and the solution was nebulized as above to form nanofibers [Figure 1]. The hybrid pSiNP/PCL nanofibers displayed average diameters ranging from 500–600 nm [Table S1, Supporting Information], and the presence of pSiNPs was confirmed by transmission electron microscopy [Figure 1], infrared spectroscopy [Figure S4, Supporting Information] and energy dispersive x-ray elemental mapping [Figure S5, Supporting Information]. The PCL fiber mats were quite hydrophobic, displaying water contact angles of 125°, and this value did not differ significantly between either the pure PCL fiber scaffolds or those composed of pSiNP/PCL [Figure S6, Table S3, Supporting Information]. The inclusion of pSiNPs in the PCL matrix also did not alter the general fiber morphology or the degree of alignment of the oriented fibers [Figure S3, Supporting Information]. Similar composite fibers could be prepared using the common biodegradable polymer PLGA in place of PCL [Figure S7, Supporting Information].

Controlling cellular growth and the direction of elongation is critical in regenerating injured tissues, especially in the nervous system where extending neurites must precisely connect across an area of injury in order to return functional use to the impacted tissues.[17, 50-52] PCL is one of a wide variety of artificial and natural materials used in constructing polymer fiber scaffolds that show efficacy in controlling and directing tissue growth.[1, 53-58] In the present case, we aimed to test the capability of the uniaxially-aligned PCL hybrid nanofibers to direct cellular extension in an *in vitro* nerve regeneration model. Whole dorsal root ganglia (DRG) were used to demonstrate the capability of the fibers to direct extending neurites. DRG were cultured on the aligned hybrid

Author Manuscript

This article is protected by copyright. All rights reserved.

nanofibers for 72 hours and imaged using fluorescence microscopy [Figure 2]. Neurons of the DRG extended neurites along the fibers, and a polar histogram of neurite growth [Figure 2e] demonstrated a strong preference for bipolar neurite extension. Control DRG cultured on flat (non-fibrous) PCL films showed no preferential directional growth of neurites.

In order to study the directed growth of single cells on the fibers, astrocytes were cultured on the aligned PCL nanofibers. Astrocytes are central nervous system (CNS) glia that are involved in synaptic maintenance, nutrient supply to neurons, neurotransmitter regulation, and several other functions of the healthy CNS.[59] They help form the glial scar following CNS injury,[60] so directing these cells with an artificial tissue scaffold holds the potential to improve neuronal regeneration by reducing scar formation at the injury borders. Astrocytes cultured on the hybrid nanofibers for 96 h exhibited good adhesion to the fibers, and they displayed a preferred orientation along the direction of fiber alignment [Figure 2]. The average angle of deviation from the median angle of cellular alignment was 6 ± 8°, whereas astrocytes cultured on control samples composed of flat PCL films showed no statistically significant preferred orientation [Figure 2e,f]. These experiments demonstrate that the aligned hybrid nanofibers created by the simple nebulization process behave similar to oriented, electrospun PCL fibers in their ability to direct the growth of single cells and the extension of growing neurites.[61-62]

Author Manuscript

This article is protected by copyright. All rights reserved.

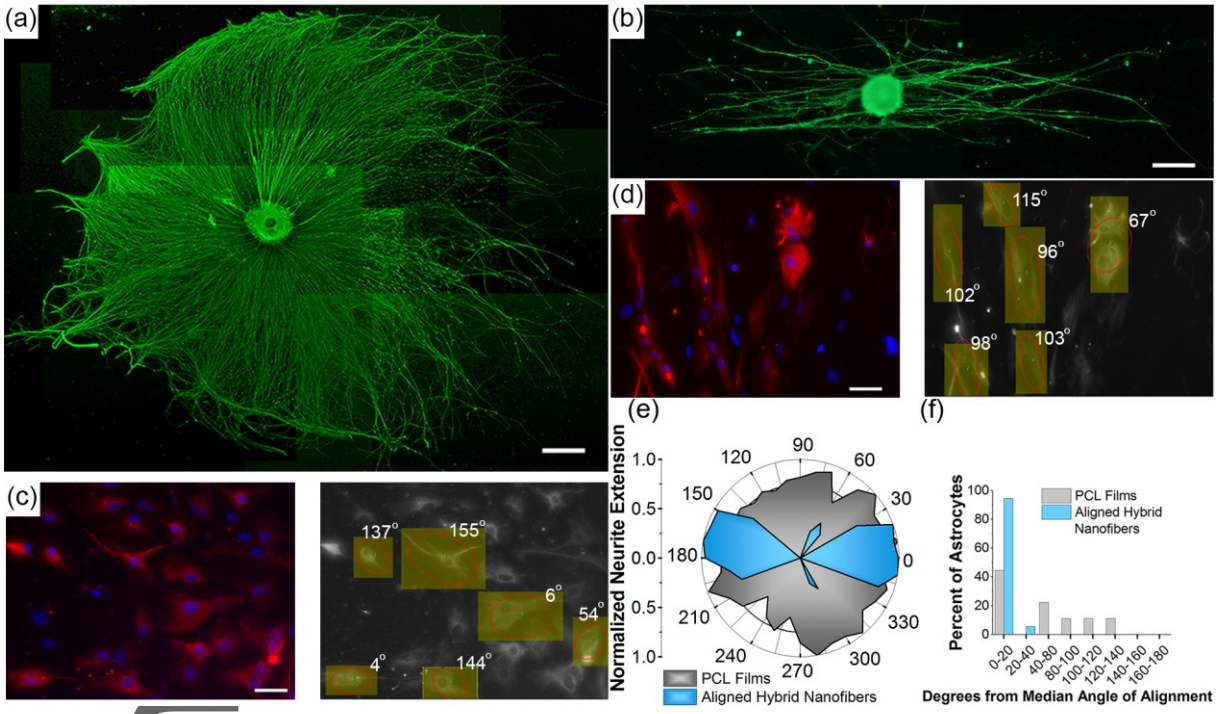

Figure 2. Fluorescence microscope image of whole rat dorsal root ganglion (DRG) stained against neurofilament (NF200) on (a) flat PCL film and (b) aligned hybrid PCL nanofibers (scale bar = 500 μm). (c) Fluorescence image of astrocytes cultured on PCL films (left image; scale bar = 50 μm, red = GFAP, blue = DAPI). Image on the right shows OrientationJ[63] analysis of astrocyte alignment superimposed on the astrocyte image, demonstrating no preferential alignment. (d) Fluorescence image of astrocytes cultured on aligned hybrid PCL nanofibers (left image; scale bar = 50 μm, red = GFAP, blue = DAPI). Image on the right shows OrientationJ analysis of astrocyte alignment superimposed on the astrocyte image, demonstrating growth along the direction of the oriented hybrid nanofibers. (e) Polar histogram of neurite extension from cultured DRG (n=3) demonstrating pronounced alignment of neurite growth along the fiber direction with the uniaxial hybrid nanofibers (blue), and no preferential alignment of neurites cultured on PCL films (gray). (f) Orientation analysis comparing astrocytes cultured on uniaxially aligned hybrid nanofibers and on flat PCL films (n=3) using OrientationJ software. Astrocytes cultured on films displayed an average angle from the median angle of alignment of 50 ± 49º, while astrocytes cultured on aligned hybrid nanofibers showed significantly greater alignment, with an average angle from the median angle of alignment of 6 ± 8º.

One important property of pSi is its photoluminescence (PL), which derives from quantum confinement effects in the silicon nanocrystallites that comprise the pSi skeleton.[64] Most

Author Manuscript

This article is protected by copyright. All rights reserved.

biodegradable polymers lack the ability to be imaged and tracked *in vivo* following implantation, and we reasoned that photoluminescent pSi embedded in the PCL nanofibers that have near-infrared (NIR) PL emission and long-lived emissive excited state could be used to confirm proper implantation and monitor scaffold degradation *in vivo.* We prepared two types of photoluminescent pSiNPs from as-etched pSiNPs: one that was loaded with the test protein lysozyme and one that was empty. The empty particles were prepared following a borate oxidation procedure that activates photoluminescence,[65] and the lysozyme-loaded pSiNPs were prepared and the luminescence activated as discussed below. Both of these preparations generated photoluminescent pSiNPs by adding a passivating silicon oxide shell to the surface of the silicon skeleton.[66-68] We found that both types of luminescent nanoparticles could be incorporated into PCL nanofibers similar to the as-etched (non-luminescent) pSiNPs. The hybrid nanofibers exhibited broad PL emission (λ_{em} = 600–1000 nm) characteristic of pSiNPs, while no PL was observed for PCL control fibers [Figure 3, Figure S8, S9, Supporting Information]. Incorporation of either the empty or the lysozyme-loaded pSiNPs into PCL nanofibers did not result in a significant change in the peak emission wavelength from the nanoparticles [Figure S8, S9, Supporting Information]. As is typical of photoluminescence from quantum-confined silicon,[69-70] the hybrid nanofibers exhibited emission lifetimes of hundreds of microseconds [Figure S8, S9, Supporting Information], and the emission half life ($T_{1/2}$) increased with increasing emission wavelength [Figure 3c].

The long emission lifetime of pSiNPs is a convenient feature for imaging of the material *in vitro* and *in vivo*, because it allows the suppression of the shorter-lived autofluorescence from endogenous organic fluorophores ubiquitous in cells, tissues, and many polymers. The time-gated method, known as Gated Luminescence Imaging of Silicon Nanoparticles (GLISiN), involves acquisition of the emission image at a time sufficiently delayed (>100 ns) from the pulsed excitation

Author Manuscript

This article is protected by copyright. All rights reserved.

such that the prompt fluorescence from the organic fluorophores has decayed to baseline and is not detected.[71] In the current experiments, a pulsed ultraviolet light emitting diode (UV LED, λ_{ex} = 365 nm) and a gate delay of 5 μs yielded microscopic GLISiN images of the pSiNP/PCL fibers with high signal-to-noise ratio (SNR) for either the empty [Figure S10, Supporting Information] or the lysozyme-loaded [Figure 3d,e] pSiNP/PCL fibers. Without time-gating, the regular fluorescence images could not distinguish autofluorescence of the PCL nanofiber controls from the pSiNP-containing fibers [Figure 3d,e, Figure S10 and Table S4, Supporting Information]. However, GLISiN images of the pSiNP/PCL fibers displayed SNR of between 20 and 80, whereas the SNR in GLISiN images of control PCL fibers (containing no pSiNPs) was < 2. Thus the GLISiN images afforded up to a 40-fold improvement in image contrast, and definitively established the presence of luminescent silicon in the fibers.

Author Manuscript

This article is protected by copyright. All rights reserved.

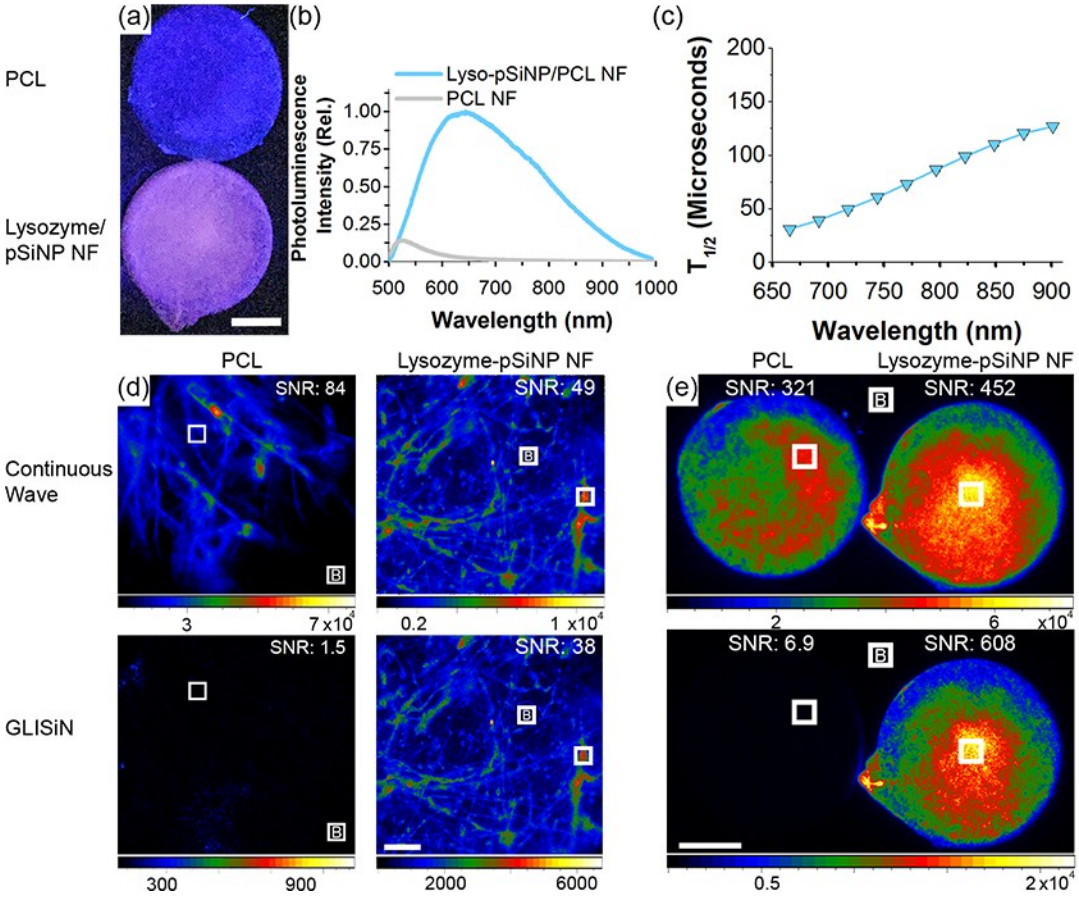

Figure 3. Steady-state and time-gated photoluminescence images of lysozyme-loaded pSiNP/PCL hybrid nanofiber scaffolds. (a) Image of PCL control (top) and hybrid nanofiber (bottom) when excited at with continuous λ_{ex} = 365 nm light emitting diode (LED) (scale bar = 5mm), and (b) corresponding emission spectra for each scaffold. (c) Photoluminescence emission half-life of the hybrid nanofiber sample (lysozyme-loaded pSiNP/PCL), measured as a function of emission wavelength, λ_{em}. Emission half-life increases with increasing λ_{em}. (d) Luminescence microscope images of control PCL fibers and lyso-pSiNP/PCL hybrid nanofibers (10x objective, λ_{ex} = 365 nm excitation, scale bar = 200 μm) obtained under steady state (continuous excitation, no time-gating) imaging conditions (top) and with time-gating (bottom). Time-gated ("GLISiN", for Gated Luminescence Imaging of Silicon Nanoparticles) images were captured using a 5 μs excitation-acquisition delay gate. Time gating removes the prompt emission and scattered light from the image. Because pure PCL has no long-lived luminescence, the GLISiN image is black. Signal-to-noise ratios (SNR) are given for the regions of interest (ROIs) indicated with the white box in each of the images (B denotes the background ROI). (e) Low magnification photoluminescence images (λ_{ex} = 365 nm, scale bar = 5mm) captured using a camera macro lens in order to survey large fields of PCL nanofibers (left) or hybrid nanofibers (right). Top two images were acquired under continuous wave excitation and bottom two images were acquired under GLISiN conditions. The GLISiN imaging parameters, SNRs and ROIs are defined as in (d).

Author MS

This article is protected by copyright. All rights reserved.

Author Manuscript

Next we evaluated the ability of the pSiNPs to protect a sensitive protein payload and enable slow release of the active protein *in vitro*. Controlled release of a biomolecule payload is of interest for inducing, enhancing, or selectively inhibiting cell growth along tissue scaffolds, and this is of particular interest in neuronal regeneration.[72] Protein-based therapeutics have posed one of the longstanding challenges in the area of drug eluting polymers, because the processing conditions used to prepare many bioresorbable polymer systems are incompatible with proteins, and the protein is often extensively denatured or hydrolyzed during formulation or during release.[73-74] For these experiments we used lysozyme as a test protein because there is a standard and sensitive assay for lysozyme activity that allows convenient quantification of denaturation or other degradative processes that the protein might undergo.[75-76] The loading procedure used for these experiments utilized a previously published phosphate buffer that oxidizes the pSiNPs, simultaneously trapping lysozyme in the pores and activating photoluminescence.[36] A bicinchoninic acid (BCA) total protein assay on the particles revealed a mass loading of lysozyme of 34 $\pm$ 1.8 %. As expected for a pore-filling process, the surface area and total pore volume of the pSiNPs decreased upon lysozyme loading [Figure S11, Table S5, Supporting Information]. The loaded protein imparted a positive overall surface charge to the pSiNPs–the zeta potential in neutral buffer increased from –22.3 $\pm$ 5.8 mV (for the empty, borate-oxidized pSiNPs) to +35 ± 2.5mV [Table S2, Supporting Information]. This increase in zeta potential upon protein loading is consistent with the pI of lysozyme (pI = 11.35),[77] indicating that the positive charge that the protein exhibits at neutral pH is imparted to the protein-loaded nanoparticles and consistent with the relatively high mass loading of protein. *In vitro* experiments indicated that the lysozyme payload was released into 37 °C, pH 7.4 buffer over a timespan of 8 days, with 55% of the protein released within the first 24 h. The

This article is protected by copyright. All rights reserved.

lysozyme enzymatic activity assay showed that the protein released into solution retained 100% of its activity throughout the period of release [Figure 4, Figure S12, Supporting Information]. Thus the protein loading process does not interfere with or degrade the function of the lysozyme payload.

Lysozyme-pSiNPs were then loaded into hybrid nanofibers by spray nebulization (3.6% by mass lysozyme, 7% by mass pSiNPs; the effective concentration of protein in polymer was 36 μg/mg) and release of the protein into 37 °C, pH 7.4 buffer was quantified for a period of 60 days [Figure 4, Figure S12, Supporting Information]. Silicon content determined by ICP-AES was 7.9 ±0.45% (Table S6, Supporting Information). Chlorine content determined by suppressed ion chromatography was 26 ±8.49 ppm for PCL control nanofibers and 101 ±13.44 ppm for lyso-pSiNP nanofibers, showing a minimal amount of chloroform retention in the nanofiber scaffolds. The buffer eluent was sampled every 3 days, and both the total mass of lysozyme (BCA assay) and the mass of active lysozyme (lysozyme enzymatic activity assay) were determined at each time point. Burst release of the drug payload, a common and generally undesired characteristic of polymeric drug delivery systems[78-80] including electrospun fibers,[81] was not observed in the present case. Only 5% of the loaded lysozyme was released in the first 9 days, and the temporal release profile was relatively constant during the first 30 days of release (corresponding to ~15% of the total protein payload released). During this period of time, activity of released lysozyme was maintained at a high level (> 90%). For the latter half of the study (days 30-60), lysozyme release slowed, and the activity of the protein released was reduced significantly. By day 60, the activity of the total lysozyme released displayed 75% of its initial activity. Approximately 1/3 of the total loaded protein had been released by day 60, and at that time the polymer fibers were still observed in the release medium.

The stability of lysozyme in these experiments did not substantially differ from what has been seen for the enzyme when stored in buffer.[82] Lysozyme showed greater stability in the

Author Manuscript

This article is protected by copyright. All rights reserved.

pSiNP/PCL nanofibers compared with many polymer and polymer fiber formulations,[10, 14] although the protein has been formulated into biodegradable polymers from water emulsion systems[83] and from water emulsion electrospinning systems[81] that displayed release and activity characteristics comparable to the present system. However, to our knowledge there are no non-aqueous routes to load active protein into polymers or polymer fibers, and the data here show that pSiNPs provide a unique means to incorporate a sensitive protein into a polymer fiber and to then deliver the active protein with a zero-order release profile for >60 days that does not display an early phase burst.

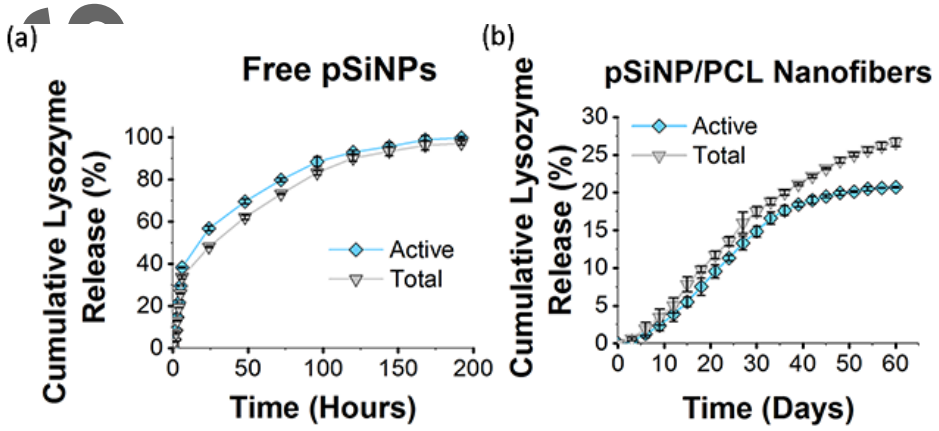

Figure 4. Cumulative percent of lysozyme released from: (a) free pSiNPs and (b) pSiNPs incorporated in PCL fibers (pSiNP/PCL nanofibers). Experiment performed in PBS buffer at 37 °C and quantified in terms of total protein (from BCA assay) and active protein (from lysozyme enzymatic activity assay). Most of the protein is released from free pSiNPs within 8 days, and nearly 100% activity is retained (a). The initial burst release of protein is suppressed, and the release of protein is substantially extended when the pSiNPs are incorporated into a PCL nanofiber scaffold (b). For the pSiNP/PCL nanofibers, less than 5% of the lysozyme payload is released in the first 9 days. The activity of released lysozyme is >90% for the first 30 days, but at later times during the release process the activity of the protein released becomes lower; by day 60 released lysozyme exhibits 75% activity (n = 3, error bars ± 3 S.D.).

The nebulization approach described here provides a simple alternative to electrospinning that can be used to fabricate aligned polymeric nanofibers capable of directing cellular growth on a

Author Manuscript

This article is protected by copyright. All rights reserved.

wide variety of surfaces, including electrical insulators. We demonstrated the incorporation of a protein delivery system based on a porous silicon host that showed superior compatibility with sensitive biologics. The ability of this system to provide sustained release of an active protein from a polymeric structure should be relevant to many advanced tissue engineering applications. The long-lived intrinsic photoluminescence originating from the silicon constituent provided an imaging feature that allows excellent rejection of signals from endogenous tissue fluorophores, providing a path for *in vivo* monitoring. We expect that the system will allow tuning of release rates and total doses of the therapeutic by adjustment of the chemistry and morphology of the pSi nanomaterial carrier and its concentration in the nanofiber matrix. Although this work only investigated a single protein, the approach is amenable to multiple drug formulations by adding different pSiNPs into the synthesis, each containing a different drug or drug combination. Due to the non-aqueous nature of the solvent used in fiber formation, the possibility of leaching or cross-contamination of water-soluble drugs during fabrication is minimized.

Supporting Information

Supporting Information is available online from the Wiley Online Library or from the author.

Acknowledgements

[II]Authors JMZ and TK contributed equally to this work. This work is supported in part by the National Science Foundation, under Grant no. CBET-1603177 (MJS) and by the National Institutes of Health, under Grant no. NINDS-RO1-NS089791 (NJA). JK acknowledges financial support from the UCSD Frontiers of Innovation Scholars Program (FISP) fellowship.

Received: ((will be filled in by the editorial staff))
Revised: ((will be filled in by the editorial staff))
Published online: ((will be filled in by the editorial staff))

Author Manuscript

This article is protected by copyright. All rights reserved.

Literature Cited:

[1] F. Yang, R. Murugan, S. Wang, S. Ramakrishna, *Biomaterials* **2005**, *26*, 2603-2610.

[2] N. Bhardwaj, S. C. Kundu, *Biotechnol. Adv.* **2010**, *28*, 325-347.

[3] Z. Ma, M. Kotaki, R. Inai, S. Ramakrishna, *Tissue Eng.* **2005**, *11*, 101-109.

[4] C. Y. Xu, R. Inai, M. Kotaki, S. Ramakrishna, *Biomaterials* **2004**, *25*, 877-886.

[5] W. J. Li, C. T. Laurencin, E. J. Caterson, R. S. Tuan, F. K. Ko, *J. Biomed. Mater. Res.* **2002**, *60*, 613-621.

[6] H. S. Yoo, T. G. Kim, T. G. Park, *Adv. Drug Deliv. Rev.* **2009**, *61*, 1033-1042.

[7] D. Liang, B. S. Hsiao, B. Chu, *Adv. Drug Deliv. Rev.* **2007**, *59*, 1392-1412.

[8] C. P. Barnes, S. A. Sell, E. D. Boland, D. G. Simpson, G. L. Bowlin, *Adv. Drug Deliv. Rev.* **2007**, *59*, 1413-1433.

[9] G. C. Ingavle, J. K. Leach, *Tissue Eng. Part B Rev* **2014**, *20*, 277-293.

[10] L. E. Sperling, K. P. Reis, P. Pranke, J. H. Wendorff, *Drug Discov. Today* **2016**, *21*, 1243-1256.

[11] R. L. Dahlin, F. K. Kasper, A. G. Mikos, *Tissue Eng. Part B Rev.* **2011**, *17*, 349-364.

[12] Y. K. Luu, K. Kim, B. S. Hsiao, B. Chu, M. Hadjiargyrou, *J. Control. Release* **2003**, *89*, 341-353.

[13] Z. C. Sun, E. Zussman, A. L. Yarin, J. H. Wendorff, A. Greiner, *Adv. Mater.* **2003**, *15*, 1929.

[14] H. L. Jiang, L. Q. Wang, K. J. Zhu, *J. Control Release* **2014**, *193*, 296-303.

[15] S. Lee, M. K. Leach, S. A. Redmond, S. Y. C. Chong, S. H. Mellon, S. J. Tuck, Z. Q. Feng, J. M. Corey, J. R. Chan, *Nature Meth.* **2012**, *9*, 917.

[16] S. S. Rao, M. T. Nelson, R. P. Xue, J. K. DeJesus, M. S. Viapiano, J. J. Lannutti, A. Sarkar, J. O. Winter, *Biomaterials* **2013**, *34*, 5181-5190.

[17] H. S. Koh, T. Yong, C. K. Chan, S. Ramakrishna, *Biomaterials* **2008**, *29*, 3574-3582.

[18] A. K. Capulli, L. A. MacQueen, S. P. Sheehy, K. K. Parker, *Adv. Drug Del. Rev.* **2016**, *96*, 83-102.

[19] J. M. Holzwarth, P. X. Ma, *Biomaterials* **2011**, *32*, 9622-9629.

[20] E. K. Purcell, Y. Naim, A. Yang, M. K. Leach, J. M. Velkey, R. K. Duncan, J. M. Corey, *Biomacromolecules* **2012**, *13*, 3427-3438.

Author Manuscript

This article is protected by copyright. All rights reserved.

18181818181818418

[21] G. A. Silva, C. Czeisler, K. L. Niece, E. Beniash, D. A. Harrington, J. A. Kessler, S. I. Stupp, *Science* **2004**, *303*, 1352-1355.

[22] Y. W. Chai, E. H. Lee, J. D. Gubbe, J. H. Brekke, *PLoS One* **2016**, *11*, e0162853.

[23] L. T. Canham, *Adv. Mater.* **1995**, *7*, 1033-1037.

[24] J. Salonen, L. Laitinen, A. M. Kaukonen, J. Tuura, M. Bjorkqvist, T. Heikkila, K. Vaha-Heikkila, J. Hirvonen, V. P. Lehto, *J. Control. Release* **2005**, *108*, 362-374.

[25] E. Tasciotti, X. W. Liu, R. Bhavane, K. Plant, A. D. Leonard, B. K. Price, M. M. C. Cheng, P. Decuzzi, J. M. Tour, F. Robertson, M. Ferrari, *Nat. Nanotechnol.* **2008**, *3*, 151-157.

[26] J.-H. Park, L. Gu, G. v. Maltzahn, E. Ruoslahti, S. N. Bhatia, M. J. Sailor, *Nature Mater.* **2009**, *8*, 331-336.

[27] S. P. Low, N. H. Voelcker, L. T. Canham, K. A. Williams, *Biomaterials* **2009**, *30*, 2873-2880.

[28] B. Godin, J. H. Gu, R. E. Serda, R. Bhavane, E. Tasciotti, C. Chiappini, X. W. Liu, T. Tanaka, P. Decuzzi, M. Ferrari, *J. Biomed. Mater. Res. Part A* **2010**, *94A*, 1236-1243.

[29] S. J. P. McInnes, T. D. Michl, B. Delalat, S. A. Al-Bataineh, B. R. Coad, K. Vasilev, H. J. Griesser, N. H. Voelcker, *ACS Appl. Mater. Interfaces* **2016**, *8*, 4467-4476.

[30] M. Kaasalainen, J. Rytkonen, E. Makila, A. Narvanen, J. Salonen, *Langmuir* **2015**, *31*, 1722-1729.

[31] H. B. Zhang, D. F. Liu, M. A. Shahbazi, E. Makila, B. Herranz-Blanco, J. Salonen, J. Hirvonen, H. A. Santos, *Adv. Mater.* **2014**, *26*, 4497-+.

[32] L. T. Canham, in *Porous Silicon for Biomedical Applications* (Ed.: H. A. Santos), **2014**, pp. 3-20.

[33] Y. Koh, S. Jang, J. Kim, S. Kim, Y. C. Ko, S. Cho, H. Sohn, *Coll. Surf. A* **2008**, *313*, 328-331.

[34] J. Kang, J. Joo, E. J. Kwon, M. Skalak, S. Hussain, Z.-G. She, E. Ruoslahti, S. N. Bhatia, M. J. Sailor, *Adv. Mater.* **2016**, *28*, 7962-7969.

[35] C.-C. Wu, Y. Hu, M. Miller, R. V. Aroian, M. J. Sailor, *ACS Nano* **2015**, *9*, 6158–6167.

[36] D. Kim, J. M. Zuidema, J. Kang, Y. Pan, L. Wu, D. Warther, B. Arkles, M. J. Sailor, *J. Am. Chem. Soc.* **2016**, *138*, 15106-15109.

[37] L. M. Bonanno, E. Segal, *Nanomedicine* **2011**, *6*, 1755-1770.

[38] W. J. Xu, R. Thapa, D. F. Liu, T. Nissinen, S. Granroth, A. Narvanen, M. Suvanto, H. A. Santos, V. P. Lehto, *Mol. Pharm.* **2015**, *12*, 4038-4047.

Author Manuscript

This article is protected by copyright. All rights reserved.

[39] Y. D. Irani, Y. Tian, M. J. Wang, S. Klebe, S. J. McInnes, N. H. Voelcker, J. L. Coffer, K. A. Williams, *Experimental Eye Research* **2015**, *139*, 123-131.

[40] A. H. Soeriyadi, B. Gupta, P. J. Reece, J. J. Gooding, *Polym. Chem.* **2014**, *5*, 2333-2341.

[41] K. Nan, F. Ma, H. Hou, W. R. Freeman, M. J. Sailor, L. Cheng, *Acta Biomater.* **2014**, *10*, 3505-3512.

[42] J. L. Coffer, in *Porous Silicon for Biomedical Applications* (Ed.: H. A. Santos), **2014**, pp. 470-485.

[43] J. L. Coffer, M. A. Whitehead, D. K. Nagesha, P. Mukherjee, G. Akkaraju, M. Totolici, R. S. Saffie, L. T. Canham, *Phys. Status Solidi A-Appl. Mat.* **2005**, *202*, 1451-1455.

[44] S. Kashanian, F. Harding, Y. Irani, S. Klebe, K. Marshall, A. Loni, L. Canham, D. M. Fan, K. A. Williams, N. H. Voelcker, J. L. Coffer, *Acta Biomater.* **2010**, *6*, 3566-3572.

[45] J. R. Henstock, U. R. Ruktanonchai, L. T. Canham, S. I. Anderson, *J. Mater. Sci.-Mater. Med.* **2014**, *25*, 1087-1097.

[46] M. A. Whitehead, D. Fan, P. Mukherjee, G. R. Akkaraju, L. T. Canham, J. L. Coffer, *Tissue Eng Part A* **2008**, *14*, 195-206.

[47] P. Mukherjee, M. A. Whitehead, R. A. Senter, D. M. Fan, J. L. Coffer, L. T. Canham, *Biomed. Microdevices* **2006**, *8*, 9-15.

[48] D. M. Fan, A. Loni, L. T. Canham, J. L. Coffer, *Physica Status Solidi a-Applications and Materials Science* **2009**, *206*, 1322-1325.

[49] W. Tutak, S. Sarkar, S. Lin-Gibson, T. M. Farooque, G. Jyotsnendu, D. Wang, J. Kohn, D. Bolikal, C. G. Simon, Jr., *Biomaterials* **2013**, *34*, 2389-2398.

[50] A. Hurtado, J. M. Cregg, H. B. Wang, D. F. Wendell, M. Oudega, R. J. Gilbert, J. W. McDonald, *Biomaterials* **2011**, *32*, 6068-6079.

[51] J. Xie, W. Liu, M. R. MacEwan, P. C. Bridgman, Y. Xia, *ACS Nano* **2014**, *8*, 1878-1885.

[52] M. Y. Gao, P. Lu, B. Bednark, D. Lynam, J. M. Conner, J. Sakamoto, M. H. Tuszynski, *Biomaterials* **2013**, *34*, 1529-1536.

[53] J. S. Choi, S. J. Lee, G. J. Christ, A. Atala, J. J. Yoo, *Biomaterials* **2008**, *29*, 2899-2906.

[54] M. Chen, P. K. Patra, S. B. Warner, S. Bhowmick, *Tissue Eng.* **2007**, *13*, 579-587.

[55] J. Venugopal, S. Ramakrishna, *Tissue Eng.* **2005**, *11*, 847-854.

Author Manuscript

This article is protected by copyright. All rights reserved.

[56] J. Venugopal, L. L. Ma, T. Yong, S. Ramakrishna, *Cell Biol. Int.* **2005**, *29*, 861-867.

[57] D. Liang, B. S. Hsiao, B. Chu, *Adv. Drug Deliv. Rev.* **2007**, *59*, 1392-1412.

[58] C. P. Barnes, S. A. Sell, E. D. Boland, D. G. Simpson, G. L. Bowlin, *Adv. Drug Deliv. Rev.* **2007**, *59*, 1413-1433.

[59] N. J. Allen, *Annu. Rev. Cell Dev. Biol.* **2014**, *30*, 439-463.

[60] J. Silver, J. H. Miller, *Nat Rev Neurosci* **2004**, *5*, 146-156.

[61] E. Schnell, K. Klinkhammer, S. Balzer, G. Brook, D. Klee, P. Dalton, J. Mey, *Biomaterials* **2007**, *28*, 3012-3025.

[62] J. Bockelmann, K. Klinkhammer, A. von Holst, N. Seiler, A. Faissner, G. A. Brook, D. Klee, J. Mey, *Tissue Eng. Part A* **2011**, *17*, 475-486.

[63] R. Rezakhaniha, A. Agianniotis, J. T. C. Schrauwen, A. Griffa, D. Sage, C. V. C. Bouten, F. N. van de Vosse, M. Unser, N. Stergiopulos, *Biomech. Model Mechan.* **2012**, *11*, 461-473.

[64] A. G. Cullis, L. T. Canham, *Nature* **1991**, *353*, 335-338.

[65] J. Joo, J. F. Cruz, S. Vijayakumar, J. Grondek, M. J. Sailor, *Adv. Funct. Mater.* **2014**, *24*, 5688-5694.

[66] V. Petrova-Koch, T. Muschik, A. Kux, B. K. Meyer, F. Koch, V. Lehmann, *Appl. Phys. Lett.* **1992**, *61*, 943-945.

[67] M. B. Gongalsky, L. A. Osminkina, A. Pereira, A. A. Manankov, A. A. Fedorenko, A. N. Vasiliev, V. V. Solovyev, A. A. Kudryavtsev, M. Sentis, A. V. Kabashin, V. Y. Timoshenko, *Sci. Rep.* **2016**, *6*, 24732-24732.

[68] B. Gelloz, N. Koshida, *Appl. Phys. Lett.* **2009**, *94*, 201903.

[69] Y. H. Xie, W. L. Wilson, F. M. Ross, J. A. Mucha, E. A. Fitzgerald, J. M. Macaulay, T. D. Harris, *J. Appl. Phys.* **1992**, *71*, 2403-2407.

[70] A. Sa'ar, *J. Nanophotonics* **2009**, *3*, 032501.

[71] J. Joo, X. Liu, V. R. Kotamraju, E. Ruoslahti, Y. Nam, M. J. Sailor, *ACS Nano* **2015**, *9*, 6233–6241.

[72] K. M. Keefe, I. S. Sheikh, G. M. Smith, *Int. J. Mol. Sci.* **2017**, *18*.

[73] K. Mader, B. Gallez, K. J. Liu, H. M. Swartz, *Biomaterials* **1996**, *17*, 457-461.

Author Manuscript

This article is protected by copyright. All rights reserved.

[74] J. Kang, O. Lambert, M. Ausborn, S. P. Schwendeman, *Int. J. Pharm* **2008**, *357*, 235-243.

[75] M. Y. Chen, M. D. Klunk, V. M. Diep, M. J. Sailor, *Adv. Mater.* **2011**, *23*, 4537–4542.

[76] J. Y. Yoon, R. L. Garrell, S. W. Choi, J. H. Kim, W. S. Kim, *Aiche J.* **2005**, *51*, 1048-1052.

[77] L. R. Wetter, H. F. Deutsch, *J. Biol. Chem.* **1951**, *192*, 237-242.

[78] S. Fredenberg, M. Wahlgren, M. Reslow, A. Axelsson, *Int. J. Pharm.* **2011**, *415*, 34-52.

[79] C. Wischke, S. P. Schwendeman, *Int. J. Pharm.* **2008**, *364*, 298-327.

[80] Y. Yeo, K. Park, *Arch. Pharm. Res.* **2004**, *27*, 1-12.

[81] Y. Yang, X. Li, M. Qi, S. Zhou, J. Weng, *Eur. J. Pharm. Biopharm.* **2008**, *69*, 106-116.

[82] A. S. Determan, J. H. Wilson, M. J. Kipper, M. J. Wannemuehler, B. Narasimhan, *Biomaterials* **2006**, *27*, 3312-3320.

[83] J. M. Bezemer, R. Radersma, D. W. Grijpma, P. J. Dijkstra, J. Feijen, C. A. van Blitterswijk, *J. Control Release* **2000**, *64*, 179-192.

Table of Contents Entry

Title: Oriented Nanofibrous Polymer Scaffolds Containing Protein-loaded Porous Silicon Generated by Spray Nebulization

Author Manuscript

This article is protected by copyright. All rights reserved.

Submitted to ADVANCED MATERIALS

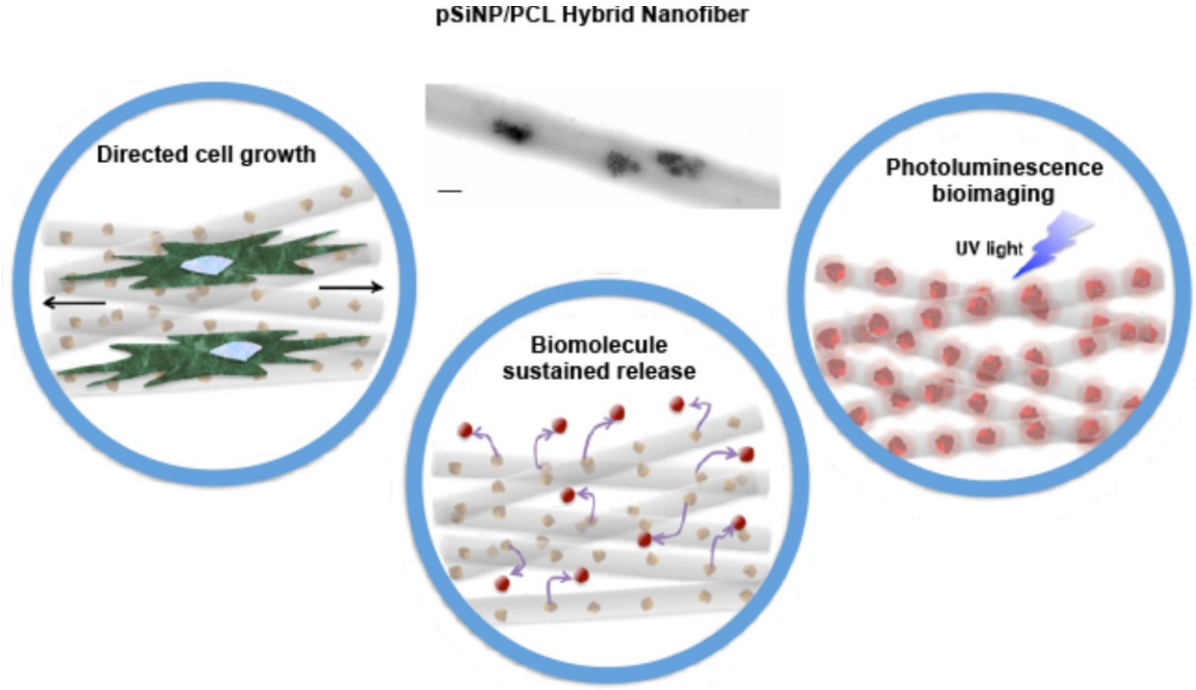

Hybrid protein-eluting nanofibers are prepared using an airbrush. The protein is sequestered in a porous silicon nanoparticle, which retains the activity of the protein and allows its deposition from a non-aqueous solvent. The fibers can be aligned to direct cellular growth , and they are capable of releasing active protein for > 60 days.

Author Man

This article is protected by copyright. All rights reserved.

23232323232323423